

# Plasmon-mediated nanofocusing beyond the diffraction limit in a visible light region through a subwavelength slit surrounded by nanogrooves

JIA-MING LIU, ZHANG-KAI ZHOU, CHONG-JUN JIN, XUE-HUA WANG\*

State Key Laboratory of Optoelectronic Materials and Technologies,  
School of Physics and Engineering, Sun Yat-Sen University, Guangzhou 510275, China

\*Corresponding author: wangxueh@mail.sysu.edu.cn

Using the Green function method, we theoretically achieve good focusing beyond the diffraction limit in a visible light region through a subwavelength slit flanked by grooves. The full width at half maximum (FWHM) of the focused spot reaches  $0.3\lambda$  ( $\lambda$  is the wavelength of incident light), which is far beyond the diffraction limited line width of  $0.5\lambda$ . The phenomena of the exceeding diffraction limit in our structure exist in the range from 500 to 630 nm. Our results can be well explained by the interference interaction between the field of the central slit and the fields penetrating through the grooves. Such image focusing will give rise to various applications in near field microscopy, lithography, high-resolution image and help to improve the design of plasmonic nanodevices.

Keywords: diffraction, surface plasmons, subwavelength structures.

## 1. Introduction

Metallic nanostructures have been the object of intensive research as they support surface plasmons, which are the collective oscillations of the electron gas in metals [1, 2]. Surface plasmons, localized and propagating in metallic nanostructure, give rise to enormous potential for light manipulating at nanoscale, field-enhanced spectroscopy, subwavelength imaging, optoelectronic devices, and chemical sensing [3–7]. The studies of functional metallic nanostructures not only broaden our fundamental understanding of photon interaction in nanosystem, but also help to build the far-reaching technological devices.

In exploration of various distinct plasmonic nanoscale applications, the extraordinary optical transmission (EOT) effect has gained extensive research efforts since its experimental discovery by EBBESEN *et al.* [8–11], and it is understood as the resonant inter-

ference coupling between the excited plasmonic waves on both surfaces of the metal films [12]. By designing various metallic structures, such as metal film with nanogrooves or subwavelength slit, it is possible to enhance light transmission as well as to modify diffraction image so as to get good nanofocusing devices [13, 14]. In fact, enormous efforts have been devoted to the development of nanogrooves structure for their fantastic nanofocusing and easy fabricated properties so as to exceed a diffraction limit in different optical regions. GRBIC *et al.* recently reported a well focusing beyond the diffraction limit at about 1 gigahertz caused by strong spatial confinement of electromagnetic waves in the near-field plate's structure [15]. MARKLEY *et al.* successfully achieved subwavelength focusing at 10 gigahertz by using a spatially shifted beam approach [16].

With the purpose of building functional imaging and spectroscopy devices, it is of great importance to extend the nanofocusing to a visible regime. But the strong near-field coupling through the metal film makes it hard to realize because the skin depth cannot be neglected [17]. Besides, light absorption and complicated manual structures are also great challenges [18]. It is not easy to fabricate subwavelength features in a large scale, and huge energy loss of visible light associated with the magnetic response exists in metallic materials [19]. Recently, some intriguing nanofocusing phenomena beyond the diffraction limit in a visible regime have been observed. WRÓBEL *et al.* got a focused spot through a concentrically corrugated silver film with the full width at half maximum (FWHM) being  $0.46\lambda$  ( $\lambda$  is the wavelength of incident light) [20]. CHEN has designed a novelty structure that can break the diffraction limit up to about 400 nm behind the output surface [21].

In this paper, we present a well visible regime nanofocusing in an easily fabricated nanostructure with a subwavelength slit and nanogrooves; the FWHM of a focused spot reaches to  $0.3\lambda$ , which is far beyond the diffraction limited line width of  $0.5\lambda$ . The strong plasmonic coupling and resonant energy transmission in our designed structure overcome the main drawbacks of light absorption and energy loss in metals, so the good nanofocusing in a visible regime can be achieved. Our findings will help to improve the design of various plasmonic devices for subwavelength focusing and high resolution image.

## 2. Theory

The material is assumed to be nonmagnetic and an  $\exp(-i\omega t)$  time dependence is used for the fields throughout the paper. One can write the wave equation of the total electric field as

$$\nabla \times (\nabla \times \mathbf{E}) - k_0^2 \varepsilon(\mathbf{r}, \omega) \mathbf{E} = 0 \quad (1)$$

where  $k_0$  is the vacuum wave number. Following MARTÍN and PILLER [22], we introduce the dielectric contrast (the subscript  $B$  means background)

$$\Delta \varepsilon(\mathbf{r}) = \varepsilon(\mathbf{r}) - \varepsilon_B(\mathbf{r}) \quad (2)$$

and the background Green function which satisfies the equation

$$\nabla \times (\nabla \times \mathbf{G}_B(\mathbf{r}, \mathbf{r}')) - k_0^2 \epsilon_B \mathbf{G}_B(\mathbf{r}, \mathbf{r}') = \mathbf{I} \delta(\mathbf{r}, \mathbf{r}') \quad (3)$$

where  $\mathbf{I}$  is the unit dyad.

According to the structure we study (Fig. 1), we choose the background to be a film (infinite in the  $x$ - $y$  plane) of thickness  $d$  embedded in the infinite space. That is the case of no slit or grooves in Fig. 1. By using this technique, we change the dif-

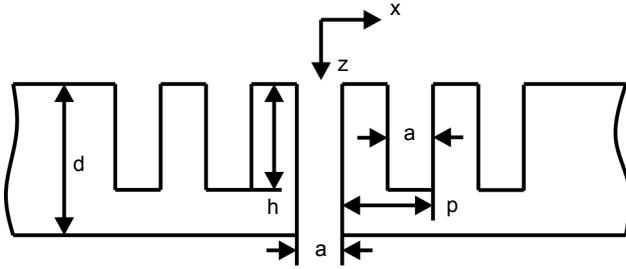


Fig. 1. Schematic picture of the structure that we study (cross-section). A slit of width  $a$  in a film of thickness  $d$  is surrounded by the grooves of the same width in the input surface symmetrically. The depth of the grooves is  $h$  and the period of the grooves is  $p$ . We set five grooves on each side of the slit.

fraction problem into a scattering problem where the slit and grooves can be seen as scatters. It will be highly efficient in calculation. The dielectric parameter of the film follows the Drude model and the data of Ag [23].

Then Eq. (1) is equivalent to the integral equation

$$\mathbf{E}(\mathbf{r}) = \mathbf{E}_B(\mathbf{r}) + \int_V d\mathbf{r}' \mathbf{G}_B(\mathbf{r}, \mathbf{r}') k_0^2 \Delta \epsilon(\mathbf{r}) \cdot \mathbf{E}(\mathbf{r}') \quad (4)$$

The integral volume is only the slit and grooves where the dielectric contrast is not zero.

The background Green function can be calculated from the electric field  $\mathbf{E}_p(\mathbf{r})$  of an oscillating point dipole  $\mathbf{p}_0$  embedded in the system at a position  $\mathbf{r}_0$  by using the relationship [24]

$$\mathbf{E}_p(\mathbf{r}) = \omega^2 \mu_0 \mathbf{G}_B(\mathbf{r}, \mathbf{r}_0) \cdot \mathbf{p}_0 \quad (5)$$

Here we divide the background into three regions by the boundary of the film. As we only need to do the integral in the slit and grooves, we set the oscillating point dipole in the middle region. Then, in each region, we have:  $\mathbf{E}_1 = \mathbf{E}_1^h, z < 0$ ;  $\mathbf{E}_2 = \mathbf{E}_2^0 + \mathbf{E}_2^h, 0 < z < d$ ;  $\mathbf{E}_3 = \mathbf{E}_3^h, z > d$ . The scattered field  $\mathbf{E}_i^h$  satisfied  $[\nabla \times \nabla \times (-k_0^2 \epsilon_i)] \mathbf{E}_i^h(\mathbf{r}) = 0, i = 1, 2, 3$ ; and  $\mathbf{E}_2^0$  is the field of an oscillating point dipole embedded in the infinite medium 2. After matching the boundary conditions

and setting three dipoles of different oscillating directions, we will get the dyad background Green function.

In this paper, we consider the situation of a plane wave being normal incident and the polarization of the electric field being along  $x$  axis. As the structure is infinite and there is no difference in  $y$  direction and the incident light is independent of  $y$ , we assume that the fields are independent of  $y$ . Then, using the Fourier expansion and with some derivation, we can rewrite Eq. (4) as

$$\mathbf{E}(\mathbf{r}) = \mathbf{E}_B(\mathbf{r}) + \frac{k_0^2(\varepsilon_0 - \varepsilon_m)}{2\pi} \int_S dS' \int_{-\infty}^{\infty} dk_x \mathbf{g}(k_x, k_y=0, z, z') \exp[ik_x(x-x')] \cdot \mathbf{E}(x', z') \quad (6)$$

where  $\varepsilon_0$  is the dielectric parameter of air and  $\varepsilon_m$  – of metal,  $\mathbf{g}$  is the Fourier transform of the background Green function,  $S$  is the cross-section of the slit and grooves. It is highly advantageous to us that only the cross-section needs to be calculated, not the whole volume.

### 3. Results and discussion

We focus our analysis on the visible and near infrared regimes. The slit width  $a$  and the thickness of the film  $d$  are set to 40 and 100 nm, respectively. As the skin depth of Ag is only tens of nanometers in the visible regime, fields cannot penetrate through the film if no groove is present. Besides, the depth of the grooves  $h$  will be a sensitivity parameter. On each side of the central slit, there are five grooves with the same width of the slit. In this case, we find that an EOT phenomena at wavelength  $\lambda = 500$  nm as well as nanofocusing beyond the diffraction limit with the grooves period  $p$  and the depth  $h$  are both 80 nm.

The transmission spectrum of the structure is shown in Fig. 2. About 4 times transmission enhancement is observed at wavelength 500 nm when the central slit is

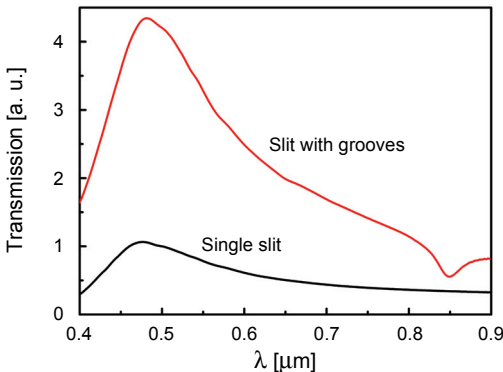


Fig. 2. Transmission spectra of the structures of single slit and slit with grooves. Here  $a = 40$  nm,  $d = 100$  nm,  $p = 80$  nm,  $h = 80$  nm, there are five grooves on both sides of the slit.

flanked by grooves, as compared to the case of only a single slit. The EOT phenomenon may be due to the surface plasmons which are excited on the input surface. It is known that the surface plasmons and quasi-cylindrical wave will be excited when light illuminates a subwavelength structure, *e.g.*, a slit or groove [25]. Furthermore, the surface plasmons or the quasi-cylindrical wave may convert into a radiant light when it reaches a subwavelength structure. So the fields in the central slit may be enhanced by the surface plasmons from the grooves surrounding it. Besides, the period grooves can supply the reciprocal vector which is needed to excite the surface plasmons [26].

The diffraction pattern of the structure at wavelength 500 nm is shown in Fig. 3a. The detection plane is set to 70 nm behind the film, with the reason that a single slit will just reach the diffraction limit ( $\lambda/2$ ) at such position. The standard is similar to Ref. [15]. For convenience, the curves are normalized. So the place with the value 0.5 at  $y$ -axis means the half maximum and we can easily compare their FWHM. The FWHM of our structure is  $0.3\lambda$  (148 nm). That is a successful subwavelength focusing beyond the diffraction limit.

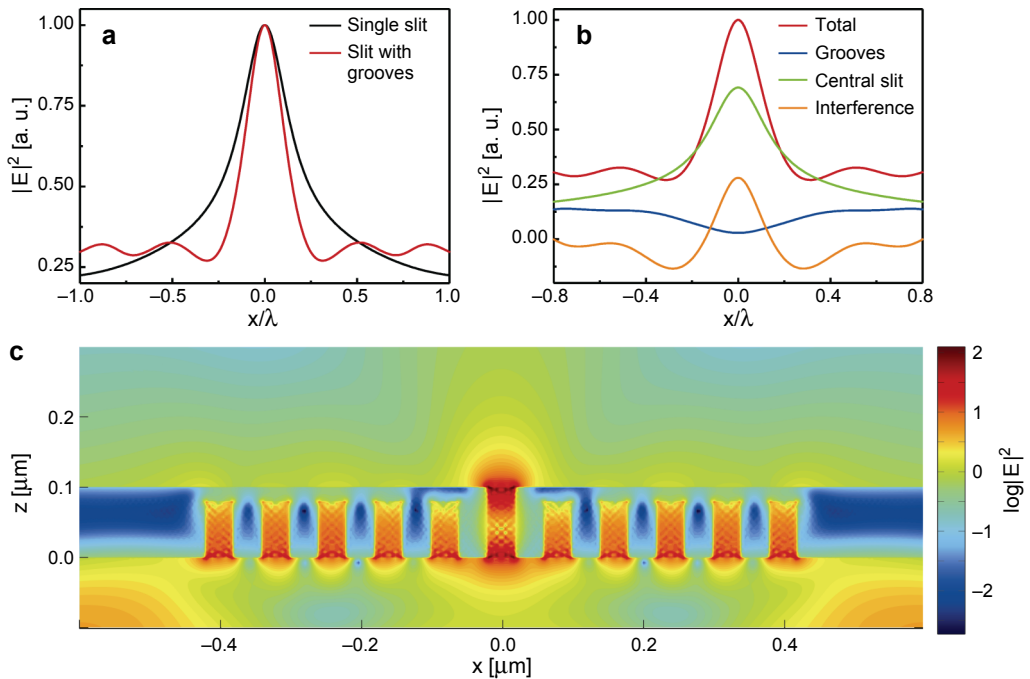


Fig. 3. (a) Diffraction images of the single slit (black) and the slit with grooves (red), the received plane is 70 nm behind the film. The curves are normalized. The FWHM in the case of the slit with grooves is  $0.3\lambda$  (148 nm) which is beyond the diffraction limit. (b) Different items contribute to the diffraction image. The red curve is the total diffraction image of the slit with grooves. The blue, green and orange curves are the contribution of the grooves, central slit and the interference between them, respectively. (c) Near field image of the case of the slit with grooves. Here  $a = 40$  nm,  $d = 100$  nm,  $p = 80$  nm,  $h = 80$  nm. The incident wavelengths are both 500 nm.

To find out the origin of the nanofocusing, we solve the near field image which is shown in Fig. 3c. The input surface of the film is set as  $z = 0$  plane, and the film area is  $0 < z < 0.1 \mu\text{m}$ . The color bar is chosen to the logarithm to the base of 10 for clear sightseeing. We observe that fields penetrate from the end of the grooves to the output side of the film. So they will influence each other and the interference with the field coming from the central slit in the output region takes place.

To confirm this idea, we make some changes in the integral equation of the Green function. Corresponding to the red curve in Fig. 3a, the norm square of the total electric field which is solved by the Eq. (6) is also shown as the red curve in Fig. 3b. For conciseness, one can also look at Eq. (4). And we will write the changed integral equations in the form of Eq. (4). After we get the fields in the slit and grooves by solving Eq. (6), we define the contribution of the grooves by confining the integral area to only the grooves

$$\mathbf{E}_{\text{grooves}}(\mathbf{r}) \equiv \int_{\text{grooves}} d\mathbf{r}' \mathbf{G}_B(\mathbf{r}, \mathbf{r}') k_0^2 \Delta\epsilon(\mathbf{r}') \cdot \mathbf{E}(\mathbf{r}') \quad (7)$$

The result of Eq. (7) is shown as the blue curve in Fig. 3b. Analogously, the contribution of the central slit is defined as

$$\mathbf{E}_{\text{slit}}(\mathbf{r}) \equiv \mathbf{E}_B(\mathbf{r}) + \int_{\text{slit}} d\mathbf{r}' \mathbf{G}_B(\mathbf{r}, \mathbf{r}') k_0^2 \Delta\epsilon(\mathbf{r}') \cdot \mathbf{E}(\mathbf{r}') \quad (8)$$

which corresponds to the green curve in Fig. 3b.

Then we define the contribution of the interference between them by

$$|\mathbf{E}(\mathbf{r})|_{\text{interference}}^2 \equiv 2\text{Re}\left(\mathbf{E}_{\text{grooves}}(\mathbf{r}) \cdot \mathbf{E}_{\text{slit}}^*(\mathbf{r})\right) \quad (9)$$

which corresponds to the orange curve in Fig. 3b.

We can see that, although the fields from the central slit have changed because of the surrounding grooves, it contributes little to the FWHM of the diffraction image. The contribution of the grooves themselves to the FWHM is also much smaller, because its value is low comparing to the contribution of the central slit. But the interference between the grooves and the central slit contributes greatly to FWHM as it has a positive value in the center to boost the peak value and some negative values in the neighboring region to cut down the spot size. So we conclude that the focusing is because of the interference between the field of the central slit and the fields penetrating through the grooves.

To further investigate the nanofocusing phenomena, we modulate the relative parameters. Figure 4a shows nanofocusing at different incident wavelengths. We observe a wide visible region (from 500 to almost 630 nm) where the FWHM is beyond the diffraction limit. The best focusing is achieved at wavelength 500 nm. It illustrates that the skin depth plays an important role in the interference between the field of the central slit and the fields penetrating through the grooves. Figure 4b shows the de-

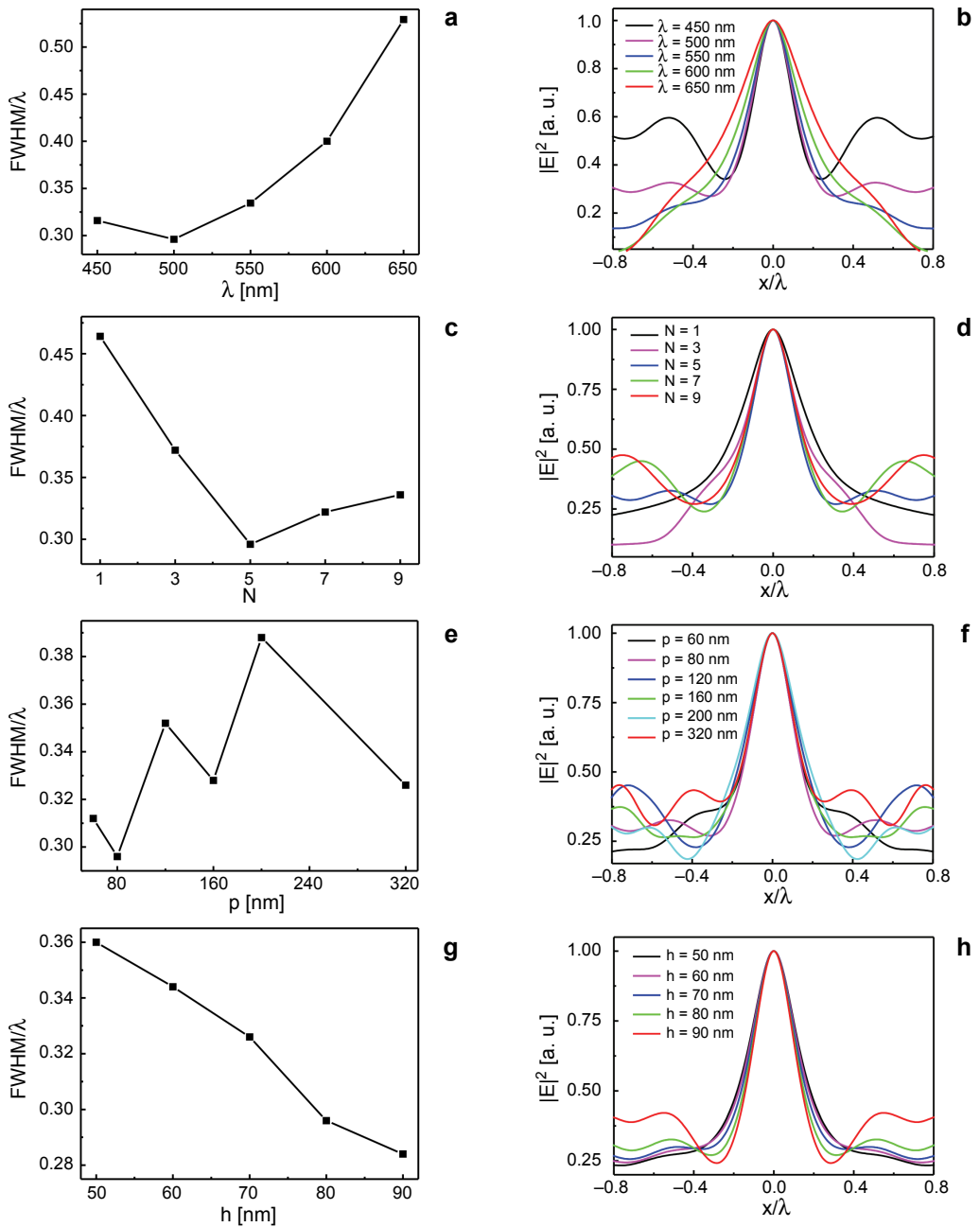


Fig. 4. FWHM as a function of different parameters. Here  $a = 40$  nm,  $d = 100$  nm. **(a)** FWHM for different incident wavelengths when  $p = 80$  nm and  $h = 80$  nm. **(b)** Diffraction image of the case of **(a)**. In **(c–h)**, the incident wavelengths are both 500 nm, and the received plane is 70 nm behind the film. **(c)** FWHM for a different number of grooves. **(d)** Diffraction image of the case of **(c)**. **(e)** FWHM for different  $p$  when  $h = 80$  nm. **(f)** Diffraction image of the case of **(e)**. **(g)** FWHM for different  $h$  when  $p = 80$  nm. **(h)** Diffraction image of the case of **(g)**. There are five grooves on both sides of the slit in **(a, b, e–h)**.

tails of diffraction images. For smaller wavelength, *e.g.*, 450 nm, deeper skin depth causes the fields much more penetrating through the grooves so that the sub-maximum is very high; on the other hand, smaller field penetration through the grooves also results in poor nanofocusing for larger wavelength.

Figure 4c shows the relationship between the number of grooves and the FWHM. In the beginning, the FWHM reduces as the number of grooves increases. But after five grooves, more grooves will not reduce the FWHM anymore or even a small increase can appear. The FWHM tends to be steady after nine grooves. Figure 4d is the diffraction image corresponding to Fig. 4c.

In Figure 4e, we change the period of the grooves while keeping the depth of the grooves  $h = 80$  nm unchanged. The trends of FWHM are similar to each other if one groove period is the power of two times the other groove period. The small period can be seemed to add a groove in the middle of the adjacent grooves of the big period. Although there are only five grooves on each sides of the central slit in Fig. 4e, however, we have proved that five grooves are enough in Fig. 4c. The detail diffraction image is shown in Fig. 4f.

Finally, in Fig. 4g, we change the depths of the grooves while keeping the period of the grooves  $p = 80$  nm unchanged. The FWHM reduces as the depth of the grooves increases. Greater depth indicates more fields penetrating through the grooves. This observation is a good evidence for our interference explanation of nanofocusing. Surely too deep grooves are not good because the affect of the sub-maximum cannot be ignored. Such as  $h = 90$  nm as it is shown by the red curve in Fig. 4h which is the diffraction image corresponding to Fig. 4g.

## 4. Conclusions

In conclusion, we achieve nanofocusing beyond the diffraction limit in the visible region from 500 to 630 nm through a subwavelength slit surrounded by nanogrooves. The FWHM of the focused spot reaches  $0.3\lambda$ , which is far beyond the diffraction limited line width of  $0.5\lambda$ . Our results can be well explained by the interference interaction between the field of the central slit and the fields penetrating through the grooves. Such subwavelength image focusing will give rise to various applications in near field microscopy, lithography, high-resolution image, and so on.

*Acknowledgements* – We thank Dr. Jingfeng Liu, Dr. Yicong Yu and Mr. Tianran Liu for helpful discussions. This work is financially supported by the National Basic Research Program of China (2010CB923200) and the National Natural Science Foundation of China (Grants 10725420, 10974263, and U0934002).

## References

- [1] SURBHI LAL, LINK S., HALAS N.J., *Nano-optics from sensing to waveguiding*, Nature Photonics **1**(11), 2007, pp. 641–648.



- [2] ATWATER H.A., *The promise of plasmonics*, Scientific American **296**, 2007, pp. 56–63.
- [3] KATAYAMA I., KOGA S., SHUDO K., TAKEDA J., SHIMADA T., KUBO A., HISHITA S., FUJITA D., KITAJIMA M., *Ultrafast dynamics of surface-enhanced Raman scattering due to Au nanostructures*, Nano Letters **11**(7), 2011, pp. 2648–2654.
- [4] NA LIU, HENTSCHEL M., WEISS T., ALIVISATOS A. P., GIESSEN H., *Three-dimensional plasmon rulers*, Science **332**(6036), 2011, pp. 1407–1410.
- [5] KASZTELANIC R., *Surface plasmon resonance sensors – novel architecture and improvements*, Optica Applicata **41**(1), 2011, pp. 145–155.
- [6] KAWATA S., ONO A., VERMA P., *Subwavelength colour imaging with a metallic nanolens*, Nature Photonics **2**(7), 2008, pp. 438–442.
- [7] ZHANG-KAI ZHOU, MIN LI, ZHONG-JIAN YANG, XIAO-NIU PENG, XIONG-RUI SU, ZONG-SUO ZHANG, JIAN-BO LI, NAM-CHOL KIM, XUE-FENG YU, LI ZHOU, ZHONG-HUA HAO, QU-QUAN WANG, *Plasmon-mediated radiative energy transfer across a silver nanowire array via resonant transmission and subwavelength imaging*, ACS Nano **4**(9), 2010, pp. 5003–5010.
- [8] EBBESEN T.W., LEZEC H.J., GHAEMI H.F., THIO T., WOLFF P.A., *Extraordinary optical transmission through sub-wavelength hole arrays*, Nature **391**(6668), 1998, pp. 667–669.
- [9] LEZEC H.J., DEGIRON A., DEVAUX E., LINKE R.A., MARTIN-MORENO L., GARCIA-VIDAL F.J., EBBESEN T.W., *Beaming light from a subwavelength aperture*, Science **297**(5582), 2002, pp. 820–822.
- [10] GARCÍA-VIDAL F.J., MORENO E., PORTO J.A., MARTÍN-MORENO L., *Transmission of light through a single rectangular hole*, Physical Review Letters **95**(10), 2005, article 103901.
- [11] HAITAO LIU, LALANNE P., *Microscopic theory of the extraordinary optical transmission*, Nature **452**(7188), 2008, pp. 728–731.
- [12] SONDERGAARD T., BOZHEVOLNYI S.I., NOVIKOV S.M., BEERMANN J., DEVAUX E., EBBESEN T.W., *Extraordinary optical transmission enhanced by nanofocusing*, Nano Letters **10**(8), 2010, pp. 3123–3128.
- [13] GARCÍA-VIDAL F.J., LEZEC H.J., EBBESEN T.W., MARTÍN-MORENO L., *Multiple paths to enhance optical transmission through a single subwavelength slit*, Physical Review Letters **90**(21), 2003, article 213901.
- [14] MARTÍN-MORENO L., GARCÍA-VIDAL F.J., LEZEC H.J., DEGIRON A., EBBESEN T.W., *Theory of highly directional emission from a single subwavelength aperture surrounded by surface corrugations*, Physical Review Letters **90**(16), 2003, article 167401.
- [15] GRBIC A., LEI JIANG, MERLIN R., *Near-field plates: subdiffraction focusing with patterned surfaces*, Science **320**(5875), 2008, pp. 511–513.
- [16] MARKLEY L., WONG A.M.H., YAN WANG, ELEFThERIADES G.V., *Spatially shifted beam approach to subwavelength focusing*, Physical Review Letters **101**(11), 2008, article 113901.
- [17] GORDON R., *Proposal for superfocusing at visible wavelengths using radiationless interference of a plasmonic array*, Physical Review Letters **102**(20), 2009, article 207402.
- [18] LINGYUN WANG, KAZUNORI HOSHINO, XIAOJING ZHANG, *Light focusing by slot Fabry–Perot photonic crystal nanoresonator on scanning tip*, Optics Letters **36**(10), 2011, pp. 1917–1919.
- [19] JIE YAO, KUN-TONG TSAI, YUAN WANG, ZHAOWEI LIU, GUY BARTAL, YUH-LIN WANG, XIANG ZHANG, *Imaging visible light using anisotropic metamaterial slab lens*, Optics Express **17**(25), 2009, pp. 22380–22385.
- [20] WRÓBEL P., PNIEWSKI J., ANTOSIEWICZ T.J., SZOPLIK T., *Focusing radially polarized light by a concentrically corrugated silver film without a hole*, Physical Review Letters **102**(18), 2009, article 183902.
- [21] CHEN K.R., *Focusing of light beyond the diffraction limit of half the wavelength*, Optics Letters **35**(22), 2010, pp. 3763–3765.
- [22] MARTÍN O.J.F., PILLER N.B., *Electromagnetic scattering in polarizable backgrounds*, Physical Review E **58**(3), 1998, pp. 3909–3915.

- [23] PALIK E.D. [Ed.], *Handbook of Optical Constants of Solids II*, Elsevier Science, USA, 1991, pp. 313–334.
- [24] TOMAŠ M.S., *Green function for multilayers: Light scattering in planar cavities*, *Physical Review A* **51**(3), 1995, pp. 2545–2559.
- [25] GUANGYUAN LI, LIN CAI, FENG XIAO, ANSHI XU, *Theoretical reexamination of the cross conversion between surface plasmon polaritons and quasi-cylindrical waves*, *Optics Letters* **35**(19), 2010, pp. 3162–3164.
- [26] GENET C., EBBESEN T.W., *Light in tiny holes*, *Nature* **445**(7123), 2007, pp. 39–46.

*Received September 29, 2012*